Simulation of a dielectric deflecting structure for short-wavelength radiation

Alexander Ody
Dept. of Applied Physics,
Stanford University
Stanford, CA 94305, USA
aody@slac.stanford.edu

R. Joel England
SLAC National Accelerator Laboratory
Menlo Park, CA 94025, USA

Zhirong Huang
SLAC National Accelerator Laboratory
Menlo Park, CA 94025, USA

***Abstract*— Recent advances on dielectric laser accelerators (DLA) have set the stage for consideration of potential applications for these devices. One such application is the use of DLA in conjunction with a dielectric deflecting structure to achieve short-wavelength radiation generation. We present a preliminary design of a deflecting structure based on previous work employing a tilted dielectric grating as a laser-driven undulator. We report the results of initial finite element and particle tracking simulations for the dielectric deflecting structure and discuss further design steps to achieve short-wavelength radiation generation.**

I. Introduction

Modern research and experiments in the field of dielectric laser acceleration (DLA) show strong promise of dielectric structures as building blocks for future accelerators [1] [2] [3]. Recent advances have motivated efforts towards future applications for DLA devices. One proposed application is the use of a tilted dielectric grating structure to excite a deflecting mode, to be used as the foundation for a laser-driven undulator [4]. The possibility for a short undulator period, set by the wavelength of the driving laser, would allow for coherent short-wavelength radiation at much lower beam energy. A dielectric deflecting structure would also allow for integration of beam steering and beam diagnostic elements driven by the same laser as the accelerating portions. Here we consider a novel scheme to excite an on-axis purely deflecting mode for relativistic electron energies.

II. Force Equations

The fields within a periodic grating structure of arbitrary rotation angle are discussed in detail in recent conference proceedings [5]. Here we consider the case of a periodic grating rotated 45 degrees about the inner axis of the channel as diagrammed in Fig 1. The forces of the resonant mode within the structure excited will take the following form:

$$F_x = -qE_0\frac{c^{\pm}}{\sqrt{2}}\begin{Bmatrix}\cosh(\Gamma y)\\ \sinh(\Gamma y)\end{Bmatrix}e^{i\mathbf{k}\cdot\mathbf{r}} \tag{1}$$

$$F_y = qiE_0\frac{c^{\pm}}{\sqrt{2}}\begin{Bmatrix}\sinh(\Gamma y)\\ \cosh(\Gamma y)\end{Bmatrix}e^{i\mathbf{k}\cdot\mathbf{r}} \tag{2}$$

$$F_z = qE_0\frac{c^{\pm}}{\sqrt{2}}\begin{Bmatrix}\cosh(\Gamma y)\\ \sinh(\Gamma y)\end{Bmatrix}e^{i\mathbf{k}\cdot\mathbf{r}} \tag{3}$$

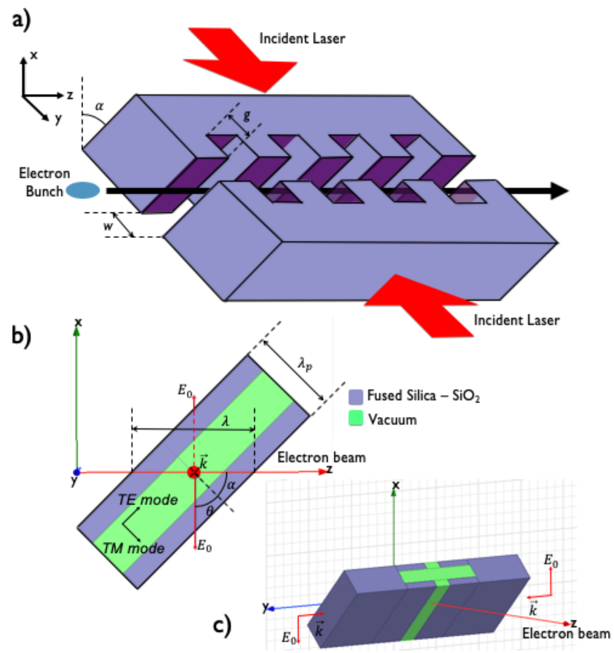

Fig. 1: **Tilted Grating Dielectric Deflecting Structure.** a) The proposed structure is a dielectric grating structure similar to current DLA structures, tilted in order to excite a deflecting mode, and dual illuminated to symmetrize the fields within the structure (see e.g. Ref. [4]). b) Cross section of one grating period of the structure in HFSS showing out-of-phase laser polarizations and electron beam axis. c) Rotated profile for perspective

TABLE I: Structure and Laser Parameters

λ	2μm	Laser Wavelength
w	0.4 λ = 800nm	Channel Width
g	0.85 λ = 1.7μm	Groove Depth
α	45°	Groove Tilt Angle
θ	45°	Laser Polarization Angle
λ_p	$\lambda\cos\alpha$ = 1.4μm	Groove Period
F_{th}	1.75 J/cm^2	Laser Fluence
τ	100 fs	Laser Pulse Duration
E_{max}	9.57 GV/m	Max Field in SiO_2

This material is based upon work supported by the U.S. Department of Energy,
Office of Science, under Contract No. DE-AC02-76SF00515.

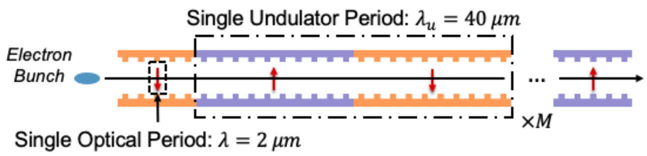

Fig. 2: **Dielectric Undulator.** Diagram of a single undulator period for a 20 grating period undulator. The grating color indicates relative injection phase, with orange and purple gratings being 180° out-of-phase relative to one another. This phase advance reverses the direction of the deflecting force in the structure every half-period. An undulator with a period of an even-integer multiple of the laser wavelength can be constructed by changing the number of grating periods per phase advance.

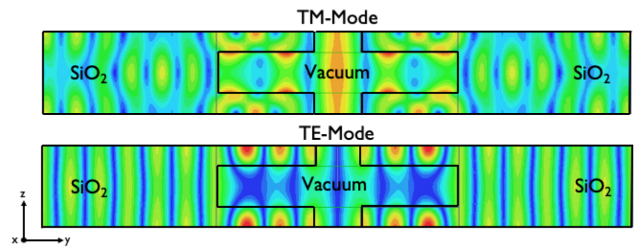

Fig. 3: **HFSS Simulation.** The simulated field magnitudes of the TE and TM electric field excitations within the structure are plotted above. The structure is illuminated on each side by 1V/m laser fields. The regions of high field strength are plotted in red, and correspond to approximately 2 V/m fields, while blue corresponds to minimal field regions tending towards 0V/m.

where the complex coefficients $c^{\pm}$ account for relative phase shifts and coupling coefficients of the excited modes. As we are considering confined modes in y, we have defined a real-valued decay constant Γ, and the upper and lower lines of each equation correspond to in-phase and π out-of-phase illumination by the lasers respectively.

At relativistic particle energies, the hyperbolic cosine dependence approaches a uniform field within the channel as the exponential decay term is much larger than the gap of the vacuum region ($w \ll \Gamma^{-1}$). Similarly, the hyperbolic sine dependence tends towards a linear function of position in the channel, passing through zero at y=0 in the center of the channel. For π out-of-phase illumination, the on axis fields in the structure take a purely deflecting form:

$$F_x = F_z = 0\,,\; F_y = q\frac{iE_0}{\sqrt{2}}c^- e^{i\kappa z} \tag{4}$$

For in-phase illumination, the particles instead experience a deflection in x as well as acceleration in z:

$$F_x = -q\frac{E_0}{\sqrt{2}}c^+ e^{i\kappa z}\,,\; F_y = 0\,,\; F_z = q\frac{E_0}{\sqrt{2}}c^+ e^{i\kappa z} \tag{5}$$

We note that off-axis, the sinh dependent terms of Eq. 3 will lead to transverse defocusing forces, which will need to be compensated for in longer structures.

III. Simulation Design

A. Structure Design

The test structure for our simulations is a laser driven undulator as diagramed in Fig. 2. Each undulator period is comprised of multiple grating periods, each one laser wavelength long. The injection phase is advanced by 180° halfway through each undulator period in order to reverse the sign of the fields within the structure. In building such a structure, this behavior can be achieved by adding a gap region half the length of an grating period. The first quarter undulator period (λ_u) of the structure couples in an on-axis electron beam. Likewise, the last quarter period straightens the outgoing beam.

B. Code Description

The fields inside the structure were first simulated using the finite-element code HFSS. A single period of the SiO_2 grating geometry (Fig. 1b) was modeled as shown in Fig. 3. The boundary conditions were defined to enforce a periodic field along the propagation axis of the channel. Two plane wave sources are set incident on the structure from each side, and the relative phases (either in-phase or π out-of-phase) were defined within the code. The TE and TM modes (both electric and magnetic) in the structure were excited, simulated, and exported individually to allow for arbitrary combination. The orthogonality of the modes allows for separate simulations. Adjusting the relative amplitude or phase of the two modes when combining the field maps is analogous to setting the rotation or ellipticity of the incident lasers' polarization.

For a chosen combination of TE and TM modes, the max electric within the SiO_2 in the combined map was located, and used to scale the fields such that the maximum field in the structure corresponded to the laser-induced damage threshold (LIDT) fluence of bulk SiO_2 in vacuum, F_{th} = 1.75 J/cm^2 [6] [7]. For a 100fs laser pulse, this corresponds to a maximum field in the structure of 9.57 GV/m.

The undulator described above is created in GPT by importing the field maps from HFSS, duplicating them, and placing them end to end to achieve the desired structure length. The injection phase of the field maps is advanced by 180° every half-undulator period as outlined above to vary the sign of the deflection force along the structure.

IV. Simulation Results

For the simulations considered here, the structure and laser parameters listed in Table I were used. Laser wavelength, λ was chosen to be 2 μm, corresponding to the wavelength of available Thulium fiber lasers. The channel width, w, and groove depth, g, are taken from optimizations for previously proposed schemes [4] and may need to be reoptimized for this new case. This will be an exercise for future work. The groove tilt angle, α, is chosen such that the forces in the TE and TM modes have identical form of Eq. 3, and the laser polarization θ is chosen to excite an equal superposition of the two modes. As stated above, the laser fluence, F_{th}, is chosen as a baseline threshold for damage in a bulk sample of SiO_2. The laser pulse duration, τ = 100fs, is typical for DLA experiments, and the corresponding threshold field in the structure is calculated $E_{max} = \sqrt{2\frac{\eta}{n}\frac{F_{th}}{\tau}}$, where $\eta = 377\Omega$ is the wave impedence of free space and $n = 1.44$ is the refractive index of SiO_2 at 2 μm.

The modes excited by E_0 = 1 V/m π out-of-phase lasers are shown in Fig. 3. The curvature in the wavefronts is a result of reflections from the periodic structure and has been observed in previous simulations of similar dielectric structures [8]. The strongest fields are located within the periodic structure, evanescing into the vacuum region between the grating teeth. For in-phase illumination by 1V/m lasers, the strongest field in the SiO_2 region of the combined field map is found to be 4.37 V/m. Similarly, the strongest field for out-of-phase illumination is found to be 2.42 V/m. The fields are scaled up in GPT to the damage threshold of 9.57 GV/m, and the corresponding incident laser fields within SiO_2 on the grating structure are thus 3.09 GV/m and 5.59 GV/m.

The structure simulated in GPT for these runs consisted of 70 grating periods as shown in Fig. 4ca. The middle 60 gratings constituted a 3 period undulator, each half undulator period being 10 grating periods long ($\lambda_u = 2 * 10 * \lambda = 40\mu m$). The first and last quarter undulator periods (each consisting of five grating periods) acted as couplers into and out of the undulator.

The parameters for the test bunch are listed in Table II. The bunch length is chosen to be sufficiently short compared to the wavelength of the laser. We are here concerned with discerning the potential undulator parameters for spontaneous undulator radiation, and will consider the effects of longer bunch lengths in forthcoming studies. We also do not here consider the effects of spacecharge or expansion due to emittance.

The electron injection phase was varied for each case (both in-phase and out-of-phase laser illumination) in order to identify a phase for maximal deflection in each case. At these maximal injection phases, the deflection of the centroid of the beam and the associated average energy modulation are plotted in Fig. 4c. We note the behavior is as predicted by Eqs. 4 & 5. For out-of-phase illumination (Eq. 4) there is primarily deflection in the confined y-direction within the channel with minimal energy modulation (Fig. 4ca), whereas for in-phase illumination (Eq. 5) there is primarily deflection in the invariant x-direction with an associated larger energy modulation (Fig. 4cb).

The motion of the particles can be compared to that of a traditional planar undulator, where the particles oscillate according to

$$y(z) = \frac{K}{\beta\gamma k_u}\sin(k_u z) \tag{6}$$

where γ is the Lorentz factor of the relativistic particles, $\beta = v/c$, $k_u = 2\pi/\lambda_u$, and K is the undulator parameter. In an undulator comprised of static magnetic fields, the undulator

TABLE II: Simulation Parameters

γ_e	100 MeV	Beam Energy
N_e	1000	Number of Electrons
$\sigma_{x,y}$	10 nm	Transverse Spotsize
τ_e/σ_z	100 as / 30 nm	Bunch Length
Q	None	Spacecharge
M_u	10	# of Grating Periods
λ_u	2 M_u λ = 40 μm	Undulator Period
M	3	# of Undulator Periods

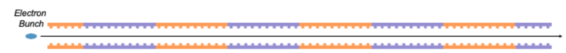

(a) (a)

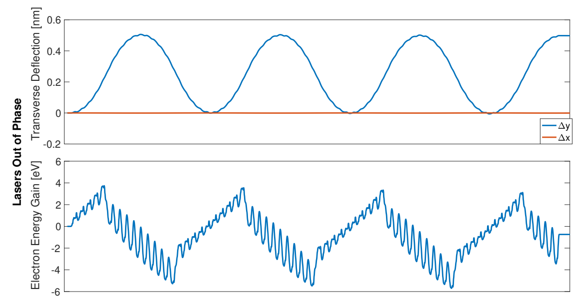

(b) (b)

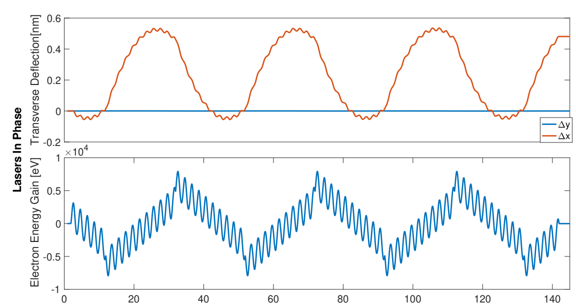

(c) **GPT Results.** The transverse deflection and energy modulation of the centroid of the beam within a three period laser-driven undulator (λ_u = 2μm) for a) out-of-phase and b) in-phase illumination. **Out-of-Phase:** The motion is primarily in the y-direction, as predicted in Eq. 4. The particles experience minimal energy modulation in the structure. **In-Phase:** As predicted by Eq. 5, the oscillation is in the x-direction, however there is an accompanying longitudinal force that results in a larger energy modulation.

parameter is related to the magnetic field, B, by

$$K = \frac{eB\lambda_u}{2\pi m_e c} = 0.934 * B[T] * \lambda_u[cm] \tag{7}$$

We can thus calculate an undulator parameter and a corresponding magnetic field for a static planar undulator that would achieve the same trajectory as our electrodynamic undulator. For out-of-phase illumination, Fig. 4ca, the trajectory is very close to sinusoidal, and the undulator parameter is calculated to be K=0.0065. The corresponding magnetic field is B=1.7T. For in-phase illumination, Fig. 4cb, the trajectory is not perfectly sinusoidal as the particles gain and lose energy through the undulator. We find the undulator parameter to be K=0.0069 and the corresponding static magnetic field to be B=1.85T.

Both the strength of the deflection force experienced by the particles and the undulator parameter are functions of injection phase, and we here report only their maximal values. Further consideration of the effects on longer bunches, which experience different undulator parameters, is left for future work.

V. DISCUSSION AND CONCLUSION

We have presented the preliminary results of our tilted-grating simulations for a 100 MeV electron beam. This energy regime is of particular interest for a potential short-wavelength radiation structure. The resonant radiation from a planar undulator has a wavelength given by:

$$\lambda_r = \frac{\lambda_u}{2\gamma^2}(1 + \frac{K^2}{2}) \tag{8}$$

If we consider a longer undulator period, λ_u = 1mm, the associated undulator parameter for out-of-phase illumination is K = 0.17. A 100 MeV electron beam ($\gamma \approx 200$) in such a structure would radiate at λ_r = 13.2 nm, within the extreme ultraviolet regime.

Simulation of the EUV radiation field produced in such a scenario will be the subject of future work and will inform planned experimental tests of this concept. Facilities for dedicated DLA experiments are expected to come online within the next year, providing access to multi-GeV test beams as well as lower energy (50 to 100 MeV) electron beams that are microbunched at the laser wavelength [9] [10]. Testing of a very short undulator section of order 1mm in length as a proof-of-concept demonstration appears feasible by simple ballistic propagation of a relativistic test beam through the ($\sim$1 micron) vacuum channel of the device. For much longer structures with more undulator periods, external focusing may be needed to compensate for defocusing forces of the undulator fields and emittance expansion of the beam [11]. Recently proposed techniques using the laser field itself to confine particles inside of laser-driven accelerators may also be useful for deflecting structures. These techniques, based on alternating phase focusing and ponderomotive harmonic focusing, have been studied numerically and are now being implemented in fabricated DLA devices and experiments [12] [13] [14].

ACKNOWLEDGMENTS

This work was supported by the Gordon and Betty Moore Foundation (GBMF4744), National Science Foundation (NSF) (PHY-1535711), and U.S. Department of Energy (DE-AC02-76SF00515, DE-SC0009914).

REFERENCES

[1] K. Wootton *et al.*, "Towards a Fully Integrated Accelerator on a Chip: Dielectric Laser Acceleration (DLA) From the Source to Relativistic Electrons," in *Proc. of International Particle Accelerator Conference (IPAC'17), Copenhagen, Denmark, 14-19 May, 2017*, no. 8 in International Particle Accelerator Conference, (Geneva, Switzerland), JACoW, May 2017. https://doi.org/10.18429/JACoW-IPAC2017-WEYB1.

[2] D. Cesar, J. Maxson, P. Musumeci, X. Shen, R. J. England, K. P. Wootton, and S. Tan, "Enhanced energy gain in a dielectric laser accelerator using a tilted pulse front laser," *ArXiv e-prints*, Apr. 2018.

[3] D. Cesar, S. Custodio, J. Maxson, P. Musumeci, X. Shen, E. Threlkeld, R. J. England, A. Hanuka, I. V. Makasyuk, E. A. Peralta, K. P. Wootton, and Z. Wu, "High-field nonlinear optical response and phase control in a dielectric laser accelerator," *Communications Physics*, vol. 1, no. 1, p. 46, 2018.

[4] T. Plettner and R. L. Byer, "Proposed dielectric-based microstructure laser-driven undulator," *Phys. Rev. ST Accel. Beams*, vol. 11, p. 030704, Mar 2008.

[5] R. J. England, A. Ody, and Z. Huang, "Transverse forces in planar symmetric dielectric laser-driven accelerators," in *Proc. of the Advanced Accelerator Concepts Workshop, Breckenridge CO*, 2018.

[6] K. Soong, R. Byer, E. R. Colby, R. J. England, and E. Peralta, "Laser damage threshold measurements of optical materials for direct laser accelerators," vol. 1507, 12 2012.

[7] K. Soong, *Particle accelerator on a wafer : demonstration of electron acceleration and diagnostics with microstructures*. PhD thesis, Stanford University, 2014.

[8] E. Peralta, *Accelerator on a chip: design, fabrication, and demonstration of grating-based dielectric microstructures for laser-driven acceleration of electrons*. PhD thesis, Stanford University, 2015.

[9] U. Dorda, R. Assmann, A. Fallahi, K. Galaydych, F. Krtner, M. B. Kuropka, W., D. Marx, N. Matlis, F. Mayet, G. Vashchenko, T. Vinatier, P. A. Walker, and J. Zhu, "The dedicated accelerator R&D facility "SINBAD" at DESY," in *Proc. of International Particle Accelerator Conference (IPAC'17), Copenhagen, Denmark, 14-19 May, 2017*, no. 8 in International Particle Accelerator Conference, (Geneva, Switzerland), JACoW, May 2017. https://doi.org/10.18429/JACoW-IPAC2017-WEYB1.

[10] R. Ischebeck, "Experimental infrastructure for dielectric laser acceleration with ultra-relativistic electron beams," in *Proc. of the Advanced Accelerator Concepts Workshop, Breckenridge CO*, 2018.

[11] A. Ody, P. Musumeci, J. Maxson, D. Cesar, R. J. England, and K. Wootton, "Flat electron beam sources for DLA accelerators," *Nuclear Instruments and Methods in Physics Research Section A: Accelerators, Spectrometers, Detectors and Associated Equipment*, vol. 865, pp. 75 – 83, 2017. Physics and Applications of High Brightness Beams 2016.

[12] U. Niedermayer, T. Egenolf, O. Boine-Frankenheim, and P. Hommelhoff, "Alternating Phase Focusing for Dielectric Laser Acceleration," *ArXiv:1806.07287 [physics.acc-ph]*, 2018. Available: https://arxiv.org/abs/1086.07287.

[13] B. Naranjo, A. Valloni, S. Putterman, and J. B. Rosenzweig, "Stable charged-particle acceleration and focusing in a laser accelerator using spatial harmonics," *Phys. Rev. Lett.*, vol. 109, p. 164803, Oct 2012.

[14] D. Cesar, P. Musumeci, and R. J. England, "All optical control of beam dynamics in a DLA," in *Proc. of the Advanced Accelerator Concepts Workshop, Breckenridge CO*, 2018.